2000

An Investigation of Two-Phase Flow in Microgrooved Tubes

T. A. Shedd
University of Illinois at Urbana-Champaign

R. Shurig
University of Illinois at Urbana-Champaign

T. Newell
University of Illinois at Urbana-Champaign

AN INVESTIGATION OF TWO-PHASE FLOW IN MICROGROOVED TUBES

Timothy A. Shedd, Robert Shurig, Ty Newell
Department of Mechanical and Industrial Engineering
University of Illinios at Urbana-Champaign
1206 W. Green St., Urbana, IL 61801

ABSTRACT

Microgrooved or microfin tubing is commonly used in refrigeration and air conditioning products because of the greatly enhance heat transfer coefficients it provides. This paper presents some results of visualization of horizontal two-phase air-water flow in clear tubing with internal grooves. Tubes of 15.2 mm inner diameter were prepared with twenty axial or helical (9 and 18 degree) grooves to allow for visualization between the grooves. Time averaged liquid film thickness and local thin film particle image velocimetry (PIV) data were obtained. These results indicate that grooves act to redistribute and thin the liquid film on the tube wall which would lead to increased heat transfer coefficients. In addition, the 18 degree helix generates the thinnest average film thicknesses in agreement with heat transfer coefficient measurements in these tubes.

INTRODUCTION

Microgrooved (also called microfin) tubes play a very significant role in modern, high-efficiency refrigerators and air conditioners. These tubes generally have about sixty 200 micron deep grooves around their inner walls which may be arranged in a variety of patterns. Currently, tubes with axial, helical and crosshatched patterns are available. With their introduction about twenty years ago, it was found that microgrooved tubes demonstrate significantly increased heat transfer coefficients over smooth tubes with only a minor addition to pressure loss. This effect is most dramatic at low mass fluxes. Yoshida et al. [1987] were the first to show that the increased heat transfer rates were primarily due to an increased heat transfer coefficient at the top of a horizontal tube. They and others theorized that this was due to liquid being wicked up from the bottom of the tube through the grooves by capillary action, thus wetting the entire tube and providing a constant, thin film for evaporation on the upper wall of the tube [Kimura and Ito, 1981]. To date, this is the only theory that has been put forward to explain the behavior of the liquid film in microgrooved tubes.

The wetting action of the grooves due to capillary action can be verified through theoretical calculations. However, these calculations indicate that this behavior should be insensitive to groove angle, while other research has determined that groove angle has a significant impact on the heat transfer in these tubes [Ito and Kimura, 1979, Kimura and Ito, 1981, Oh and Bergles, 1998]. In addition, one model constructed on the basis of capillary wetting consistently underpredicts the heat transfer coefficient in flows where the capillary effect should be dominant [Shikazono et al., 1998]. Hence, although this previous work shows that capillary action is significant, heat transfer data suggests that it is not the only, or even the dominant, behavior driving the more uniform wetting of the tube wall.

To better understand the behavior of two-phase vapor-liquid flow in horizontal microgrooved tubes, flow visualization experiments were performed in clear tubes with microgrooves using air and water. An optical film thickness measurement system and thin film particle image velocimetry (PIV) were used to better understand the nature of the liquid film flow. The results of these experiments clearly indicate that the grooves significantly influence the distribution of the liquid film.

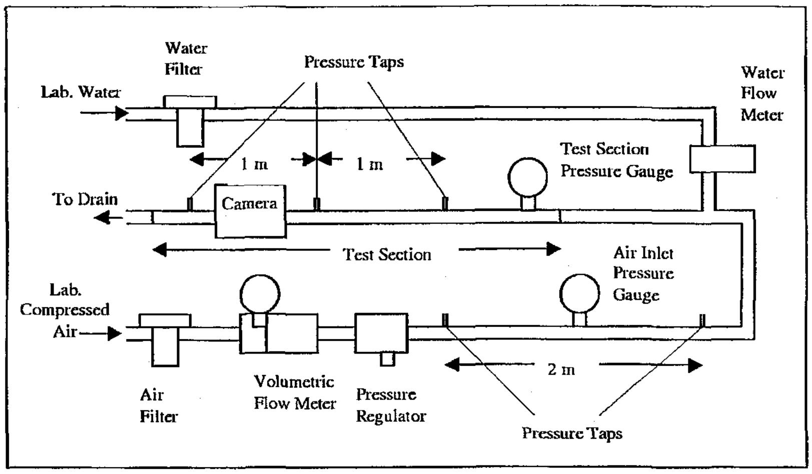

Figure 1: Experimental air/water test loop.

EXPERIMENTAL SETUP

The primary experimental apparatus is shown in Figure 1. Laboratory compressed air is regulated and passed through a 3 m entrance tube. The mass flow rate of the air is determined by measuring the pressure drop across this entrance tube. The Colebrook correlation for friction factor along with the definitions of friction factor, Reynolds number and mass flow rate are then solved simultaneously to provide the mass flow rate of air in the loop. This process is simplified by using the Engineering Equation Solver (EES) from F-Chart Software. Water from the laboratory main passes through a rotameter volumetric flow meter before entering the test section through a coarsely porous wall. Both the water and air are filtered to 5 microns prior to entering the apparatus.

Pressure gradients are measured using solid state differential pressure transducers. The inlet pressure transducer has a sensitivity of ± 1.7 Pa while the test section transducers are sensitive to ± 6.8 Pa. Gauge pressures in the entrance and test sections were monitored with bourdon gauges.

The test sections were constructed of 0.5 inch schedule 40 clear PVC tubing. The actual inner diameter of the tubes was 15.2 mm. The total observable length was about 6.1 m including a 3.1 m smooth flow development section. The grooved test sections were fabricated by pulling the tubes over a die with four orthogonal cutting points which were set to cut grooves 200 microns deep. A guide sleeve slotted with the appropriate helix angle was used to rotate the tube during the cutting. This process was manual and prone to some inconsistency; the resulting grooves were not perfectly spaced nor as smooth as production quality copper tubes. In addition, only 20 grooves (as opposed to 60 in commercial tube) were cut into each tube to allow space for visualization between the grooves. In spite of these differences, the resulting data show trends that correspond to heat transfer observations made in commercial copper and aluminum tubing.

Name	$\dot{m}_g$ kg/s	$\dot{m}_l$ kg/s	Ft	x	G kg/sm^2
T	0.0048	0.0032	70	0.6	44
U	0.0067	0.0032	120	0.68	55
V	0.0099	0.0032	210	0.76	73
Q	0.0047	0.0063	50	0.42	61
R	0.0079	0.0063	105	0.56	79
F	0.0110	0.0063	165	0.64	97
G	0.0152	0.0063	250	0.71	120

Table 1: Details of the experimental flow conditions.

Local liquid film thicknesses were obtained using an optical measurement system described by Shedd and Newell [1998]. The time averaged liquid film thicknesses presented here were measured to within ± 0.010 mm. Some flows appeared to have some long time period (spanning more than 15 minutes) fluctuations causing local film thickness variations of 0.03 to 0.06 mm, however these were not studied in detail. The film thicknesses were measured at about 390 L/D from the point where liquid was introduced. However, the actual grooved length of the test section varied due to the nature of their fabrication. Film thickness was measured at 170 L/D, 140 L/D and 120 L/D from the beginning of the 0, 9 and 18 degree grooved sections, respectively.

PIV was performed by injecting spherical glass beads into the liquid flow right before it entered the test section. These beads appeared to have a mean diameter of about 0.06 mm. The particles were illuminated using a stroboscope at 418 Hz and recorded in digital video using a Sony DCRTRV-510 video camera with a close-up lens. Images were selected and processed to eliminate the background structure. Finally, PIV interrogation was performed using the PIV Sleuth software package [Christensen and Soloff, 2000]. For more details on PIV, the reader is referred to Adrian [1991],Keane and Adrian [1992] and Oakley et al. [1997].

The flow conditions tested are shown in Table 1.

RESULTS

Figure 2 plots the friction factors of the various tubes against the vapor Reynolds number. This plot reaffirms that the presence of grooves only generates a mild increase in pressure loss over smooth tubes in two phase annular flow.

Liquid film thickness profiles for four different flows are shown in Figure 3. The smooth tube profiles are essentially symmetrical left to right, but show the effects of gravity with thicker liquid on the bottom. Contrast with these the profiles of the helically grooved tubes. First, the thickest parts of these films has been rotated counterclockwise (the same direction as the groove helix), so it would appear that these films are symmetrical about a line passing through the center of the tube at some angle from upper left to lower right. Second, the amount of wetted tube periphery is substantially increased. In the lowest flow approximately 62% of the dry tube is wetted versus 81% of the 9 degree and 94% of the 18 degree tubes.

Finally, note that the film thicknesses of the 18 degree tube are generally smaller than all of the rest. This is shown more clearly in Figure 4 where the average film thickness for each tube and flow condition is plotted versus the Froude rate. The Froude rate is a non-dimensional group that essentially represents the ratio of the rate of kinetic energy flowing in the vapor to the power required to pump liquid from the bottom to the top of the tube at its axial flow rate.

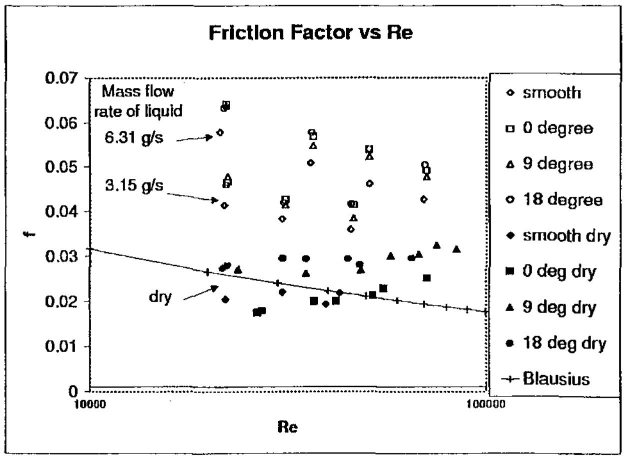

Figure 2: Friction factor versus Reynolds number for various flow conditions in the four different tubes.

It is defined by

$$\begin{aligned}
\mathrm{Ft} &= \sqrt{\frac{\dot{m}_g}{\dot{m}_l}}\mathrm{Fr} \\
&= \sqrt{\frac{\dot{m}_g}{\dot{m}_l}}\left(\frac{U_{sg}}{\sqrt{gd}}\right) \qquad (1)\\
&\sim \frac{\text{gas phase power}}{\text{liquid phase pumping power}},
\end{aligned}$$

where the subscript g and l represent vapor and liquid quantities, respectively, U_{sg} is the superficial vapor velocity (the velocity of vapor if it occupied the entire tube at the same mass flow rate), g is the gravitational acceleration and d is the tube diameter. Ft has been found to be a useful parameter for correlating some two-phase flow quantities. [Hurlburt and Newell, 2000, Yashar et al., 2000]

The liquid film thickness profiles in the axially grooved tube are not remarkable as they tend to follow the smooth tube profiles very closely.

To better understand the forces involved in maintaining the time averaged film thickness profiles, an investigation into local liquid velocities and turbulent statistics is under way using a novel PIV implementation. Figures 5 and 6 show local velocity vectors in a disturbance wave and the same location 30 ms later. This vertical upflow within the disturbance wave has been observed in the past using laser dye activation [Sutharshan et al., 1995] and a smooth tube liquid film flow model constructed around it [Fukano and Ousaka, 1989], however, detailed information such as this has never before been available. This system will also allow for the determination of local turbulence statistics that have not been available for liquid film flows as thin as these.

DISCUSSION

The results presented indicate that one of the primary reasons for the increased heat transfer coefficients in helically microgrooved tubing is a redistribution of the liquid film resulting in thinner, more uniform films on the tube wall. In addition, these results appear to verify that

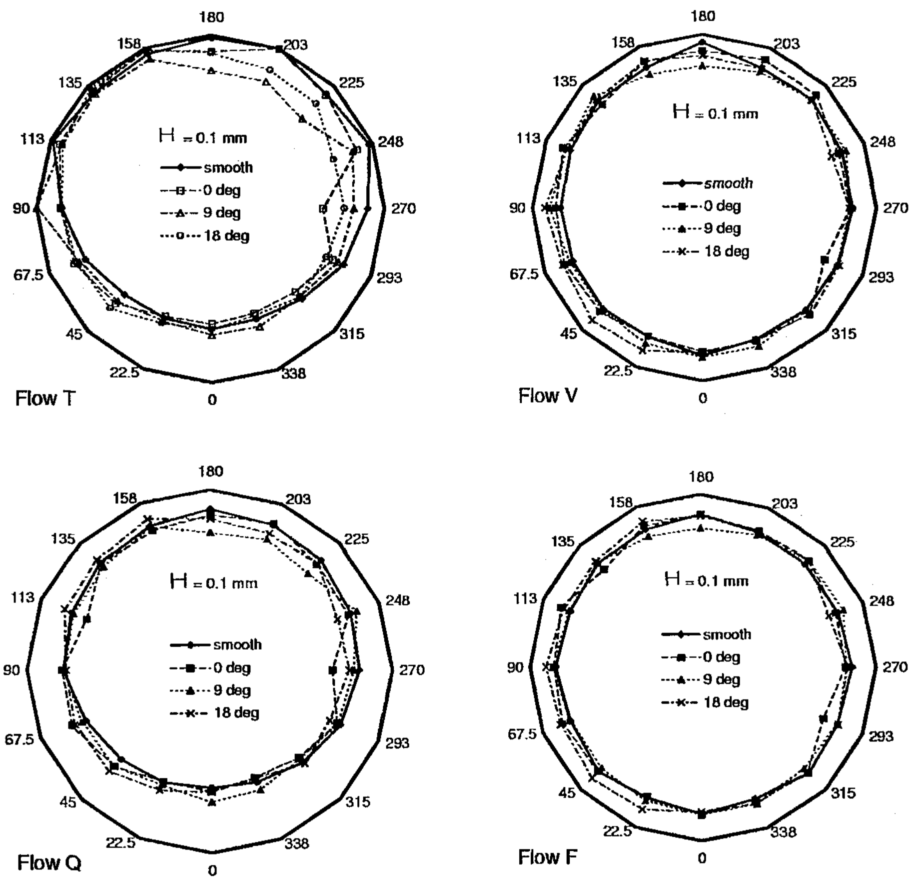

Figure 3: Time average liquid film profiles for four different flow conditions. The flow conditions are defined in Table 1. Note that these plots are not to scale for better comparison. Some distortions are artifacts of this scaling.

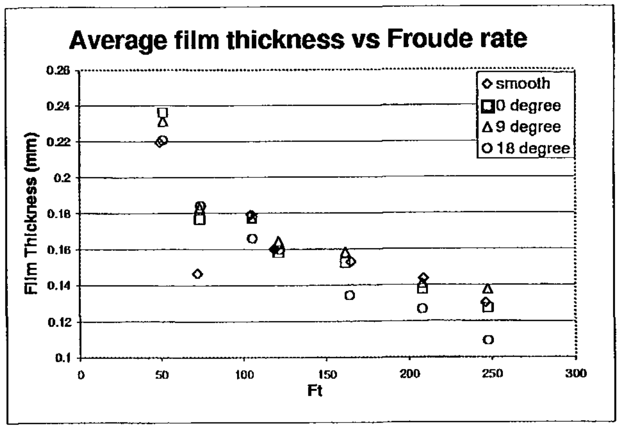

Figure 4: Average circumferential film thickness versus Froude rate (Ft).

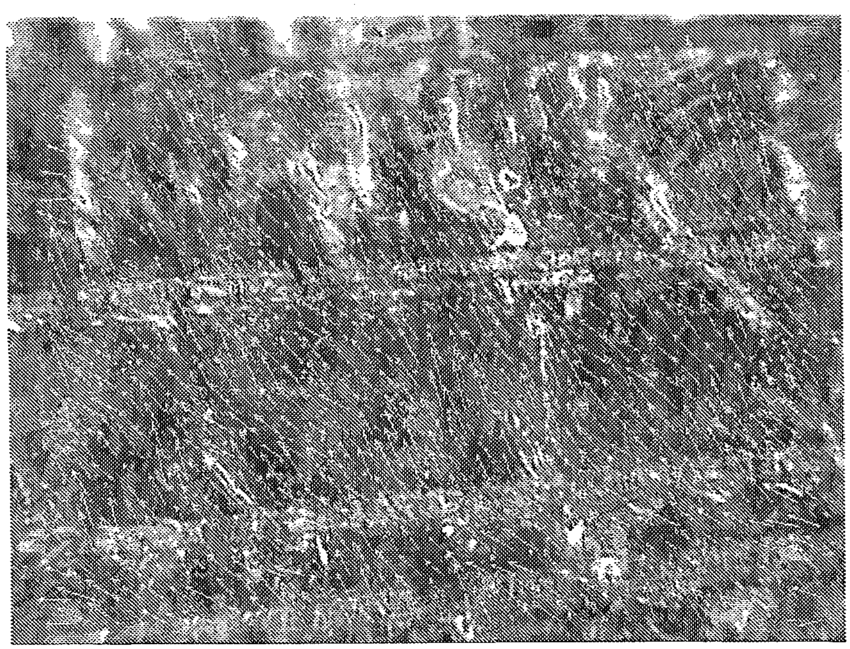

Figure 5: Local liquid film velocities of flow Q within a passing disturbance wave obtained by thin film PIV. The mean upward velocity is approximately 0.2 m/s.

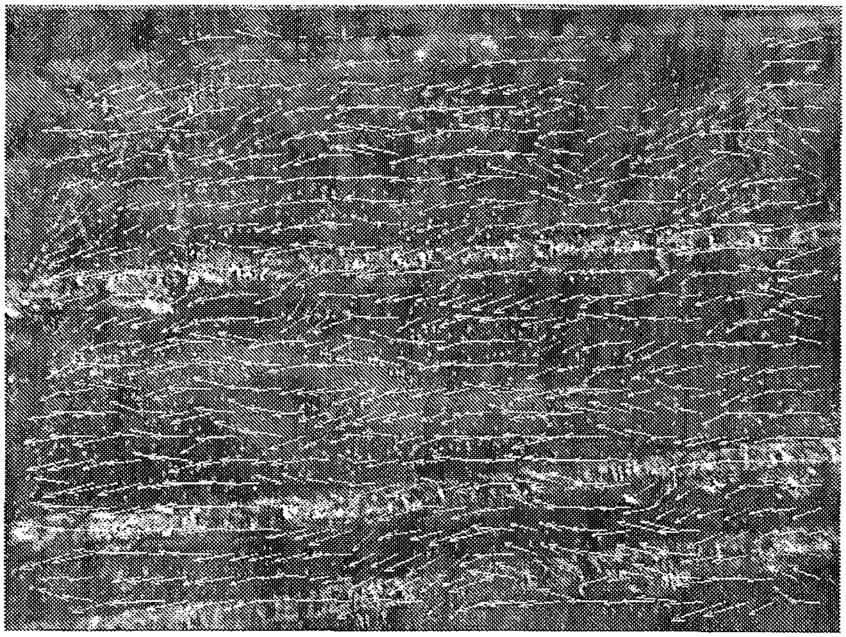

Figure 6: Local liquid film velocities 30 ms after the previous image was taken. The mean velocity to the left is approximately 0.1 m/s.

tubes with the 18 degree helix will perform better due to the fact that the liquid is somehow thinned in these tubes to a greater extent than in others.

In addition, the PIV results clearly show that the turbulent disturbance waves play an important role in maintaining an annular liquid film in horizontal tubes. However, the flow in between waves appears to be nearly laminar and does not appear to follow the groove direction closely.

While more data are needed to analyze this problem, it seems that one possible explanation for the liquid redistribution is that the grooves act on a thin layer of liquid next to the wall, perhaps like a viscous sublayer in a Law of the Wall type of velocity profile, which, in turn, applies a circumferential shear stress to the remaining liquid.

Further PIV analysis together with film thickness measurements of different fluids in these tubes as well as tubes with helix angles greater than 18 degrees will provide the basis for a sound theoretical model describing two-phase flow in horizontal microgrooved tubes.

ACKNOWLEDGMENTS

The authors gratefully acknowledge the support of the Air Conditioning and Refrigeration Center of the University of Illinois at Urbana-Champaign under projects 77 and 113. Thanks to Cyndra Lattimore, Audrey Miller and Colleen Dewey for assistance with the experimental apparatus.

References

R J Adrian. Particle–imaging techniques for experimental fluid mechanics. *Annual Review of Fluid Mechanics*, 23:261–304, 1991.

K T Christensen and S M Soloff. PIV Sleuth: Integrated particle image velocimetry (PIV) aquisition/interrogation/validation software. See http://lctf.tam.uiuc.edu for more information.

T Fukano and A Ousaka. Prediction of the circumferential distribution of film thickness in horizontal and near-horizontal gas-liquid annular flows. *International Journal of Multiphase Flow*, 15(3):403–419, 1989.

E T Hurlburt and T A Newell. Prediction of the circumferential film thickness distribution in horizontal annular gas-liquid flow. *Journal of Fluids Engineering, Transactions of ASME*, 122:1–7, 2000.

M Ito and H Kimura. Boiling heat transfer and pressure drop in internal spiral-grooved tubes. *Bulletin of the JSME*, 22(171):1251–1257, 1979.

R D Keane and R J Adrian. Theory of cross-correlation analysis of piv images. *Applied Scientific Research*, 49:191–215, 1992.

H Kimura and M Ito. Evaporating heat transfer in horizontal internal spiral-grooved tubes in the region of low flow rates. *Bulletin of the JSME*, 24(195):1602–1607, 1981.

T R Oakley, E Loth, and R J Adrian. A two-phase cinematic PIV method for bubbly flows. *Journal of Fluids Engineering – Transactions of the ASME*, 119:707–712, sep 1997.

S Y Oh and A E Bergles. Experimental study of the effects of the spiral angle on evaporative heat transfer enhancement in microfin tubes. *ASHRAE Transactions*, 104(2):1137–1143, 1998.

T A Shedd and T A Newell. Automated optical liquid film thickness measurement method. *Review of Scientific Instruments*, 69(12):4205–4213, Dec 1998.

N Shikazono, M Itoh, M Uchida, T Fukushima, and T Hatada. An analytical model to predict the condesation heat transfer coefficient in horizontal microfin tubes. *ASHRAE Transactions*, 104(2):143–152, 1998.

B Sutharshan, M Kawaji, and A Ousaka. Measurement of circumferential and axial liquid film velocities in horizontal annular flow. *International Journal of Multiphase Flow*, 21(2):193–206, 1995.

D A Yashar, M J Wilson, H R Kopke, D M Graham, J C Chato, and T A Newell. An investigation of refrigerant void fraction in horizontal, microfin tubes. *To be published in HVAC& R Research*, 2000.

S Yoshida, T Matsunaga, H P Hong, and K Nishikawa. Heat transfer to refrigerants in horizontal evaporator tubes with internal, spiral grooves. In P J Marto, editor, *Proceedings of the 1987 ASME-JSME Thermal Engineering Joint Conference*, volume 5, pages 165–172, 1987.